



Original software publication

StrutSurf: A tool for analysis of strut morphology and surface roughness in additively manufactured lattices

Reece N. Oosterbeek*, Jonathan R.T. Jeffers

Department of Mechanical Engineering, Imperial College London, London, SW7 2AZ, United Kingdom



ARTICLE INFO

Article history:

Received 14 October 2021

Received in revised form 8 February 2022

Accepted 6 March 2022

Keywords:

Additive manufacturing

Micro-strut

Lattice material

Surface roughness

ABSTRACT

Additively manufactured lattice materials are of great interest in many applications, however the surface defects generated during manufacturing can prove a significant barrier. The small feature size and intricate geometry makes characterisation of lattice struts difficult, so we present StrutSurf as a new tool for analysis of lattice struts. Using micro-CT data, StrutSurf allows random sampling of struts within a lattice, and automates analysis to provide detailed morphological information such as strut diameter, ellipticity, orientation, and surface roughness. StrutSurf will enable a range of new research questions to be investigated such as the effects of surface treatments and other manufacturing methods on strut morphology and roughness.

© 2022 Published by Elsevier B.V. This is an open access article under the CC BY license (<http://creativecommons.org/licenses/by/4.0/>).

Code metadata

Current code version

Permanent link to code/repository used for this code version

Code Ocean compute capsule

Legal Code License

Code versioning system used

Software code languages, tools, and services used

Compilation requirements, operating environments & dependencies

If available Link to developer documentation/manual

Support email for questions

v1.0

<https://github.com/ElsevierSoftwareX/SOFTX-D-21-00197>

GNU GPL v3 or later

git

MATLAB, MATLAB add-ons Optimization Toolbox and Image Processing

Toolbox, iso2mesh toolbox.

Installation using MATLAB runtime, source code can be compiled in MATLAB

<https://github.com/ReeceOosterbeek/StrutSurf>r.oosterbeek@imperial.ac.uk

1. Motivation and significance

The rise of 3D printing as a manufacturing technique has opened up a wide variety of material architectures for exploitation. Strut-based lattices are particularly promising, with a range of structures based on BCC, FCC, and other unit cells and variants possible, as well as pseudorandom and stochastic strut-based lattices [1–4]. These all provide enormous possibilities for designing new material properties, with the ability to introduce tailored functionalities by topology optimisation, controlled anisotropy, and functionally graded structures [5–9]. Advances in these areas have potential applications in medical implants, lightweight aerospace or automotive components, and energy absorption materials [10–13].

The main disadvantage of these materials is often the defects generated during the additive manufacturing process. These depend on the exact manufacturing method used: for the powder bed fusion (PBF) methods often used for metallic 3D printing this includes semi-sintered or non-melted particles, while high roughness and layer defects like weld lines are also common to many additive manufacturing techniques [14]. These defects have a significant effect on the resulting mechanical properties, acting as stress concentrators and crack initiation sites, reducing the static mechanical strength and the fatigue lifetime [15,16]. The latter is a crucial problem, and a central factor that has held additively manufactured components back from widespread adoption.

Several methods for surface treatment of additively manufactured struts have been investigated, including chemical etching, electrochemical polishing, and sand blasting [17–19]. These studies show qualitative improvements in surface quality, and as

* Corresponding author.

E-mail address: r.oosterbeek@imperial.ac.uk (Reece N. Oosterbeek).

a result demonstrate considerable increases in fatigue performance, however are not able to quantify the changes in surface topography. This is due to the inherent limitations of conventional techniques for roughness measurement such as optical or contact profilometry, which rely on line-of-sight to measure 2D surfaces. Measuring the internal surface topography within a 3D porous lattice requires alternative methods such as micro-CT, which utilises X-rays that can penetrate through the structure. Some micro-CT data analysis software packages include a wall thickness function, which allows the average strut thickness to be determined [20,21], however this discards much information about the detailed strut morphology and surface topography. To measure strut roughness from micro-CT data, Kerckhofs et al. demonstrated and validated a protocol which extracts a line profile from a micro-CT cross section, which can be used to calculate various roughness parameters [22,23]. However, reducing the 3D strut to a line profile in this way could introduce error based on the orientation of the strut and choice of sectioning plane, and discards much of the 3D data regarding the strut shape and surface topography. Du Plessis et al. [21] suggest that characterisation of nonflat surfaces can be carried out by fitting a geometric shape to the micro-CT data, and determining the deviation at each point, but this functionality typically requires proprietary software and is more comparable to CAD-based variance rather than fitting an arbitrary function. The latter is particularly important as additively manufactured micro-struts can often deviate from the intended circular cross-section resulting in an elliptical-prism shaped strut [24]. With improvements in AM resolution, micro-strut lattices are also becoming more prevalent [25,26]. These can contain several thousand struts within a single part [24,27], which can make manual inspection of micro-CT data and region selection challenging and prone to bias.

StrutSurf aims to make use of all the 3D information that micro-CT provides to determine the detailed strut morphology, and extract the full (areal) surface roughness. This will enable geometric parameters such as diameter (semi-major and semi-minor for elliptical cross-sections, maximum and minimum Feret diameter) and build angle to be measured, and the surface roughness of the strut surface (S_a , S_q , S_z) to be assessed. In addition to detailed strut analysis, other factors such as appropriate sampling must be considered in the measurement of lattice struts. StrutSurf aims to ensure representative sampling by allowing randomised generation of regions within a dataset, so that a statistical sample of struts can be built up to represent the lattice structure.

The future of additively manufactured lattice materials will require significant technical challenges to be overcome, one of the most critical of which is the need to improve the surface finish of struts by altering manufacturing parameters or by post-processing methods. Quantifying the effect of these changes is difficult for established surface measurement techniques, so alternatives such as micro-CT are necessary. These methods are increasingly being adopted [21–24], however micro-CT data analysis software that meets the specific needs of strut morphology and roughness analysis is currently lacking. StrutSurf will meet this need, allowing easier and more quantitative analysis of lattice strut morphology and surface roughness, and contribute to the development of new lattice-based materials for applications from aerospace components to medical implants.

2. Software description

StrutSurf is written in MATLAB [28], and makes use of the MATLAB add-ons Optimization Toolbox and Image Processing Toolbox. It also relies on the open-source iso2mesh toolbox for mesh generation developed by Fang et al. [29,30]. StrutSurf is provided as an executable installer that requires the (free) MATLAB Runtime library, or as MATLAB source code that can be

executed within MATLAB. Data analysis using StrutSurf involves the following steps, as illustrated in Fig. 1:

- Import binarised micro-CT image slices
- Generate a region of interest (ROI) centred around a point within the 3D dataset, which can be either manually or randomly selected
- Create a mesh of the structure within this ROI
- User positions a cylindrical mask over the strut to be analysed
- Automated analysis extracts this strut and performs the desired analysis steps
- Tabulated results and plots can be saved and exported by the user

StrutSurf is operated from the main GUI window, which has separate tabs for importing data, sampling regions, masking a strut, and viewing/exporting analysis results. From the import tab the user can select and import a micro-CT dataset, which can then be viewed along different axes using MATLAB's inbuilt slice-Viewer. The imported dataset must be in binary (i.e. black and white) image format, which can be generated after segmentation by standard micro-CT analysis/reconstruction software, or using tools such as Fiji/ImageJ [31]. Imaging additively manufactured lattices at the resolution required for characterisation of surface roughness results in a very large dataset, such that generating a mesh that maintains this resolution is impractical. The sample region tab allows the user to select a smaller region of interest for analysis. These regions can be randomly sampled based on a selection of algorithms (to achieve uniform sampling density across a certain geometry) or added manually to allow reproduction of previous analyses. A mesh of this region of interest is then generated using the binsurface function within iso2mesh [29,30]. The mask tab allows the user to position a mask around a selected strut for analysis, and select the geometry to fit to the strut (either cylindrical or an elliptical cylinder).

When the analysis procedure is begun, the ROI mesh is cropped to the portion within the cylindrical mask. Non-linear least squares regression is used to fit a cylindrical geometry to the strut, with the initial values and solver limits being based on the user-defined mask. If an elliptical cylinder is chosen as the fit geometry, then this fitted cylinder is used as the initial starting point for further non-linear least squares regression of the ellipse geometry. Once the desired geometry has been fitted, the surface is “unwrapped” from this geometry to determine the deviation from this fitted shape. For a cylindrical fit this can be calculated analytically in a straightforward way using the perimeter of a circle, while for an elliptical cylinder this is carried out by numerically integrating an incomplete elliptic integral of the second kind. Once this planar surface has been extracted from the curved strut and resampled to an even grid, areal surface roughness parameters can be calculated including the average roughness (S_a), root-mean-square roughness (S_q) and maximum peak to trough roughness (S_z). These parameters are calculated as defined in ISO 25178-2 [32]. The final results table then presents the dataset name and parameters required to reproduce the analysis (ROI position and size, masking parameters), strut characteristics (distance from centre, elevation angle, fitted diameter, Feret diameter), and calculated roughness values, which can all be saved to file and updated. To simplify calculations and prevent errors, all values are given in pixel units, and can then be converted by the user to SI units by multiplying by the pixel size. To generate plots in SI units the pixel size can be entered by the user, but this only affects visualisations and not the calculated results data table.

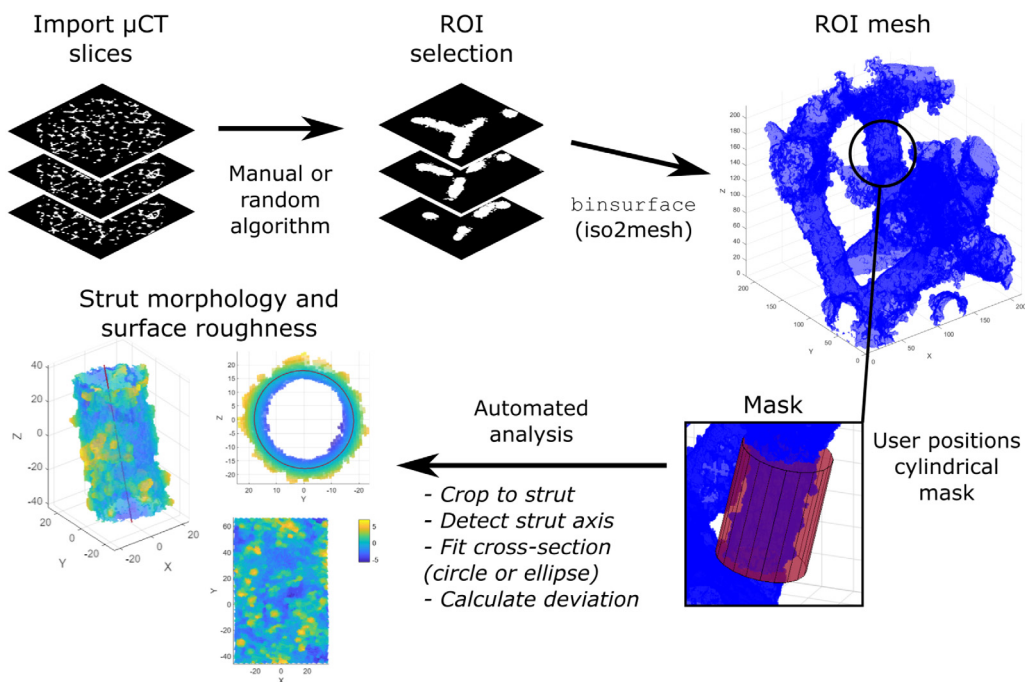


Fig. 1. StrutSurf workflow, showing importing of micro-CT data, ROI selection and meshing, masking of a strut, and analysis results.

3. Illustrative examples

3.1. Materials and methods

The lattice samples used in this example were designed in Rhinoceros 6.0 (Robert McNeel & Associates) using a method described previously [4,7]. Briefly, a random distribution of points was generated in a $\varnothing 13 \text{ mm} \times 22 \text{ mm}$ cylindrical volume; these points were then joined by zero thickness lines. Lines with a build angle of $<25^\circ$ were split into two parts and redrawn in a 'kinked' configuration such that the strut connects the same points but kinks upwards to increase the angle of the strut to the build plate to $\geq 25^\circ$ to ensure successful fabrication, as described by Hossain et al. [7]. The resulting lattices had an average connectivity of 5.8 and strut concentration of 4.1 mm^{-3} . The custom-built Imperial College Lattice Slicer was used to generate slices and assign laser parameters from the line representation using a $70 \text{ }\mu\text{m}$ contour. The lattice was fabricated using an AM250 metal powder bed fusion (PBF) system (Renishaw plc., UK) using CP-Ti powder with particle size range $10\text{--}45 \text{ }\mu\text{m}$ ($D_{50} = 27 \text{ }\mu\text{m}$) supplied by Carpenter Additive (Widnes, UK). Build parameters used were: $50 \text{ }\mu\text{m}$ layer thickness, 50 W laser power, $50 \text{ }\mu\text{m}$ point distance, and $240\text{--}500 \text{ }\mu\text{s}$ exposure time for a nominal strut diameter of $240 \text{ }\mu\text{m}$, resulting in a relative density of 13.6%. Micro-CT data was collected using a Zeiss Xradia 510 Versa, with X-ray voltage and current of 140 kV and $72 \text{ }\mu\text{A}$, with 2401 projections (0.15° spacing) and 5 s exposure, and a pixel size of $6.26 \text{ }\mu\text{m}$. Image projections were reconstructed into 3D datasets using the Scout-and-Scan software (Zeiss), and thresholding (Otsu) was applied using Fiji [31] to generate binary images for use by Strutsurf.

3.2. Analysis in StrutSurf

The following examples were generated on a laptop computer with an Intel Core i7 quad-core 1.3 GHz processor, 16 GB RAM, and 2 GB Nvidia GeForce MX350 graphics card. After binarisation the micro-CT dataset used was 8 GB in size, and was loaded into StrutSurf within 200 s. Other computational steps (generating ROI mesh, strut analysis using cylindrical or elliptical cylinder

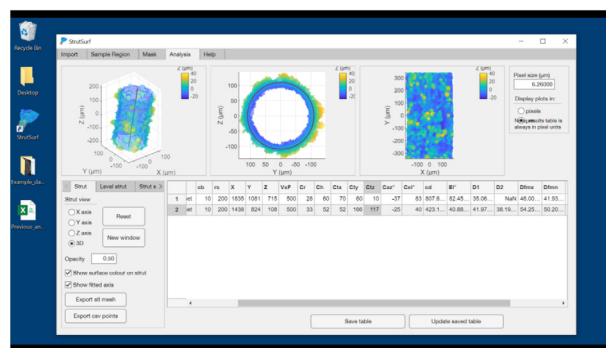


Fig. 2. Explanatory video demonstrating the use of StrutSurf to analyse lattice strut morphology and surface roughness. For video see Appendix A. Supplementary data.

fit) were completed in less than 10 s each. These examples are described below and demonstrated in the supplied explanatory video in Fig. 2.

3.3. Single strut morphology

StrutSurf can be used to gather detailed information about the morphology of individual lattice struts. A randomly generated ROI is shown in Fig. 3, with a cylindrical mask placed over the strut selected for analysis. After positioning the mask, analysis can be completed automatically using the “Analyse Strut” button. Fig. 4 shows analysis results for this strut, at approximately 41° elevation angle located approximately 2.7 mm radially from the centre of the lattice. Using an elliptic cylinder fit it can be seen that the strut has a slight eccentricity, with diameters along the semi-major and semi-minor axes of 263 and 239 μm respectively. This gives an elliptical ratio ($D2/D1$) of 1.10, comparable to results from Hossain et al. [24]. Other parameters such as the maximum Feret diameter (340 μm) and average surface roughness ($S_a = 10.6 \mu\text{m}$) can also be obtained.

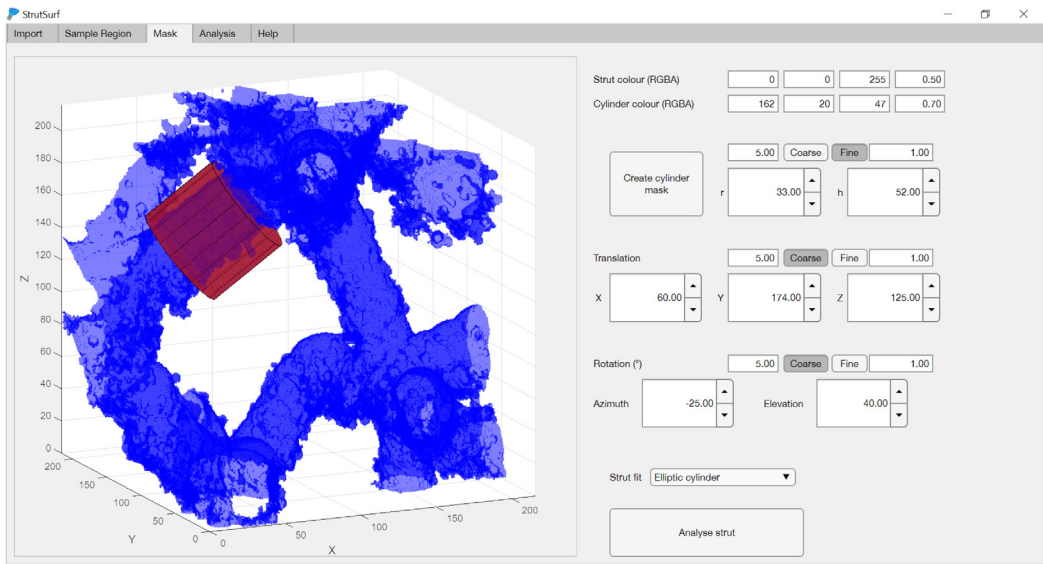


Fig. 3. Screenshot of StrutSurf mask tab showing a cylindrical mask positioned over a selected strut within a randomly generated ROI.

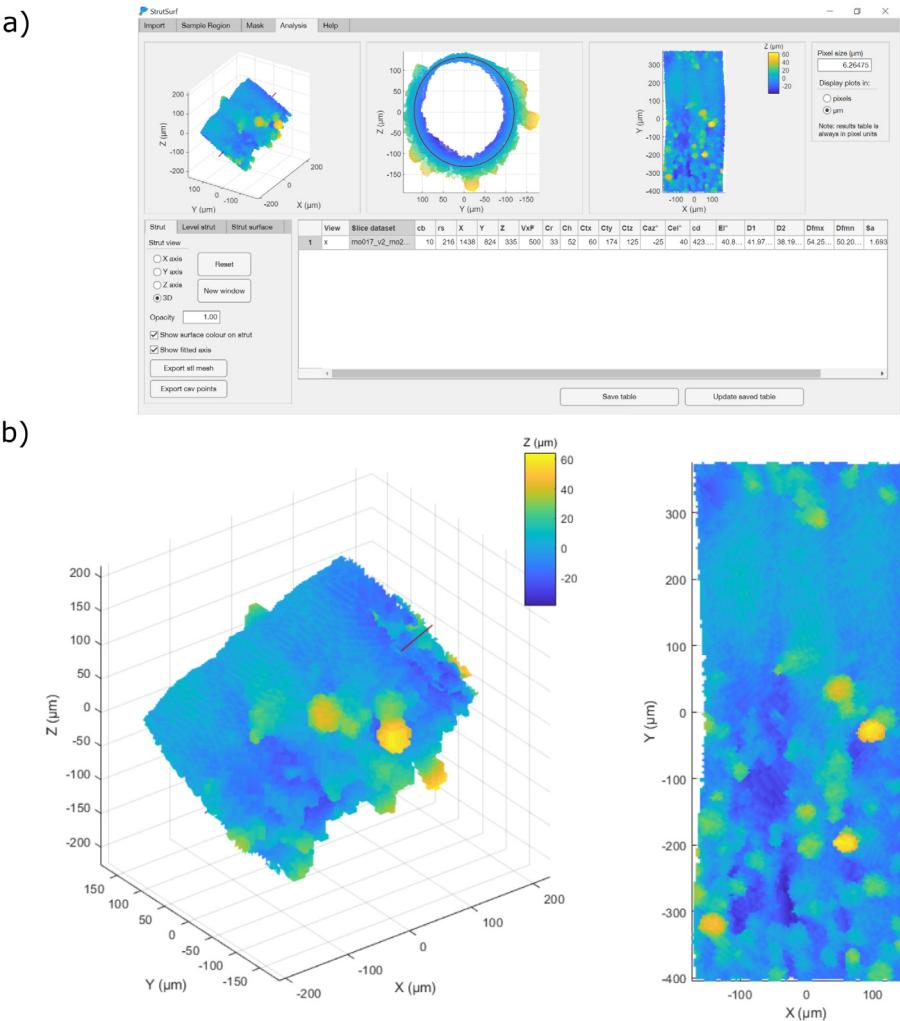


Fig. 4. Analysis results for a selected strut, showing (a) screenshot of StrutSurf analysis tab and (b) exported 3D plots of the strut and extracted surface.

In addition to these parameters it is interesting to observe the variation in morphology across the strut surface. Fig. 4a (middle) shows the strut with its axis aligned to the x-axis; here the top

surface of the strut corresponds to $z > 0$, while the underside of the strut corresponds to $z < 0$. On the extracted surface plot (Fig. 4b right) these correspond to $y > 0$ and $y < 0$ respectively.

From the extracted surface plot it is clear that the underside of the strut has considerably higher roughness than the upper surface due to semi-fused particles adhering to the strut – this is a common phenomenon observed in PBF processes when producing overhanging geometries. By comparison the upper surface is smoother, with few semi-fused particles visible, although gradual height variation is visible due to weld lines between layers. Using this surface data extracted by StrutSurf we now have the ability to quantitatively assess the roughness on the top and bottom surfaces of the strut, with S_a values of $7.45\ \mu\text{m}$ (top) and $12.64\ \mu\text{m}$ (bottom) confirming previous qualitative observations.

3.4. Lattice analysis

If a larger number of ROIs are generated, and struts analysed, data generated by StrutSurf can be used to investigate the properties of the lattice as a whole. This example shows data gathered from 50 different struts from different ROIs generated within the same lattice. ROIs were randomly generated using the “Cylinder: Radially uniform” option, to randomly sample points within the lattice, with the random distribution being uniform over r , the radial distance from the centroid of the dataset. Fig. 5 shows the variation in the surface roughness (S_a) measured for these 50 struts.

As the build angle increases the surface roughness is seen to decrease, as a result of the mechanism discussed above, where production of overhanging geometry leads to adhesion of semi-fused particles. Here we see this is consistent not just for a single strut but a sample of the whole population. Fig. 5 also shows that there is no observable correlation between surface roughness and the distance from the lattice centre. This is as expected for an as-built lattice, however this type of analysis may be valuable for assessing surface treatment methods, where the effect depth is of crucial importance.

4. Impact

With additive manufacturing becoming a more prominent technology in both research and industrial manufacturing, new technologies are needed in many areas to support advanced research and applications. In this case, additively manufactured strut-based lattice materials are an important area that utilises the unique capabilities of AM to fabricate novel structures for a variety of applications. Especially in the case of metal PBF, the surface quality of these struts is of paramount importance for their eventual application, with the mechanical and biological properties of the materials highly dependent on the morphology and surface roughness.

Due to the importance of these properties, there is increasing research interest in measuring the surface quality of additively manufactured micro-struts. However, due to the challenges associated with analysis of struts within a complex lattice, these investigations are mostly limited to representative single struts [24,33]. This can provide valuable information about the surface quality and morphology of as-built struts, although there are many cases where a single strut cannot be representative of all struts within a lattice. Most importantly, when assessing surface treatment methods the lattice as a whole must be considered, as the penetration of any surface treatment method into the lattice is a key limiting factor. To date few studies have attempted to conduct measurements of surface quality throughout a lattice, and these have been limited to extraction of 2D line profiles [22, 23].

StrutSurf allows easy selection and analysis of struts, even when contained within a complex lattice structure, and extracts the full surface profile of the selected strut. This will enable new

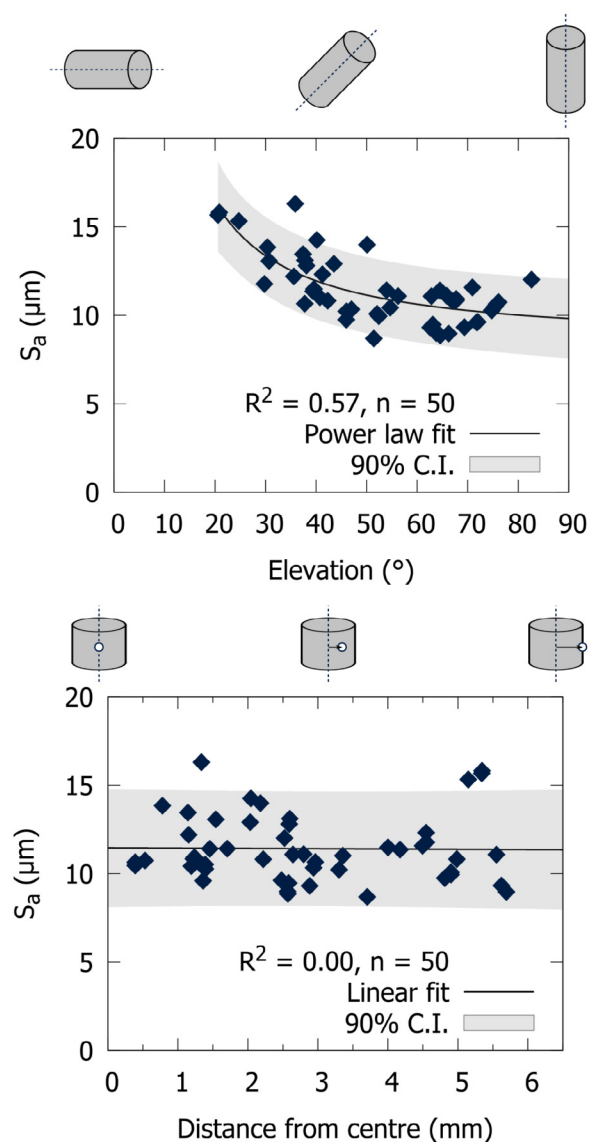


Fig. 5. Variations in measured average surface roughness for struts within a lattice, shown across elevation angle (top) and distance from centre (bottom). Trendlines were fitted using MATLAB cftool, and are displayed as a guide for the reader.

quantitative research into the surface structure of lattice micro-struts, and the effects of any treatment procedure on this surface. Surface treatment and finishing of additively manufactured parts is a burgeoning field with a diverse range of new techniques emerging. Although lattices are challenging for many of these methods progress is being made, and analysis solutions such as StrutSurf will be critical to assessing the effects of these methods.

In addition to detailed strut surface information, StrutSurf can also fulfil a similar role to existing wall thickness algorithms for routine strut thickness measurement. While existing methods provide a bulk measure averaged across the whole lattice, StrutSurf samples individual struts and can therefore provide more detailed information such as ellipticity and variations in strut thickness within the same lattice. This capability will be particularly useful in applications such as functionally graded lattice materials and assessing print quality. Within the authors' research group StrutSurf is now being used for routine analysis of additively manufactured lattice materials, enabling accurate measurements of strut diameter even with relatively low resolution

micro-CT data. The distinct advantages of StrutSurf in quantifying surface roughness are also critical to forthcoming research on the effect of certain surface treatments on the surface roughness and resulting mechanical properties of lattice materials.

It should be noted that, as with most data analysis tools, the analysis technique cannot overcome poor data quality. Lower resolution micro-CT scans (i.e. large pixel/voxel size) can be sufficient for strut thickness measurements, but for quantification of surface roughness and topography higher resolution is necessary, such that features influencing roughness (in these examples semi-fused particles) can be reliably resolved. Pixel size is not the only factor however, and other aspects of image quality also have an important role. Critically, a high contrast low noise image is required to ensure that thresholding (not carried out in StrutSurf) provides an accurate representation of the material surface. StrutSurf does contain functionality for removing small disconnected objects that can result from image noise, but this cannot remove noise artefacts that alter the strut surface.

One limitation of this technique is the requirement to manually position a mask over a strut for analysis (Fig. 3), which requires non-trivial user input. Methods for automatically detecting lattice features have recently been presented [34,35], however these focus on nodes and leverage the periodic nature of regular lattices. Methods applicable to non-regular arbitrary geometries would be a valuable future development and could be incorporated into a later version of StrutSurf in order to automate analysis further and save user time.

5. Conclusions

This paper presents the software StrutSurf, a tool to analyse strut morphology and surface roughness within additively manufactured lattice materials. StrutSurf imports an acquired micro-CT dataset, and generates randomly sampled regions of interest within this dataset. The user positions a mask over the strut to be analysed, and the software performs automated detection of strut axis, fitted geometry, and extraction of surface topography. StrutSurf complements existing wall thickness algorithms for measuring strut thickness by allowing more detailed and direct measurement of variations in strut thickness within a single lattice. It also provides new functionality by making possible extraction of the full surface topography and resulting roughness parameters for a single strut. Research interest in additively manufactured strut-based lattices is growing, however the mechanical (especially fatigue) and biological properties of these materials are inhibited by their morphology and surface roughness. StrutSurf can play a central role in the future of this field, enabling new investigations of strut roughness and morphology, and allowing the effects of surface treatments and other manufacturing methods to be studied in detail.

Declaration of competing interest

The authors declare that they have no known competing financial interests or personal relationships that could have appeared to influence the work reported in this paper.

Acknowledgements

The authors would like to acknowledge Mr Stelios Kechagias and Mr Morgan Nightingale for their assistance in testing the software, Dr Umar Hossain for helpful initial discussions, and Dr Shaaz Ghouse and Mr Edward Spiers for building the Imperial College Lattice Slicer software. The authors wish to gratefully acknowledge support from the Engineering and Physical Sciences Research Council, United Kingdom (EP/R042721/1), Wellcome Trust, United Kingdom (208858/Z/17/Z), and National Institute for Health Research, United Kingdom (NIHR300013).

Appendix A. Supplementary data

Supplementary material related to this article can be found online at <https://doi.org/10.1016/j.softx.2022.101043>.

References

- [1] Mazur M, Leary M, Sun S, Vcelka M, Shidid D, Brandt M. Deformation and failure behaviour of ti-6al-4v lattice structures manufactured by selective laser melting (SLM). *Int J Adv Manuf Technol* 2016;84(5–8):1391–411.
- [2] Mullen L, Stamp RC, Fox P, Jones E, Ngo C, Sutcliffe CJ. Selective laser melting: A unit cell approach for the manufacture of porous, titanium, bone in-growth constructs, suitable for orthopedic applications. II. Randomized structures. *J Biomed Mater Res - B Appl Biomater* 2010;92(1):178–88.
- [3] Deshpande VS, Fleck NA, Ashby MF. Effective properties of the octet-truss lattice material. *J Mech Phys Solids* 2001;49(8):1747–69.
- [4] Ghouse S, Babu S, Van Arkel RJ, Nai K, Hooper PA, Jeffers JR. The influence of laser parameters and scanning strategies on the mechanical properties of a stochastic porous material. *Mater Des* 2017;131:498–508.
- [5] Loh GH, Pei E, Harrison D, Monzón MD. An overview of functionally graded additive manufacturing. *Addit Manuf* 2018;23:34–44.
- [6] Plocher J, Panesar A. Review on design and structural optimisation in additive manufacturing: Towards next-generation lightweight structures. *Mater Des* 2019;183:108164.
- [7] Hossain U, Ghouse S, Nai K, Jeffers JR. Controlling and testing anisotropy in additively manufactured stochastic structures. *Addit Manuf* 2021;39:101849.
- [8] Zhang XY, Fang G, Leeftang S, Zadpoor AA, Zhou J. Topological design, permeability and mechanical behavior of additively manufactured functionally graded porous metallic biomaterials. *Acta Biomater* 2019;84:437–52.
- [9] Maietta S, Gloria A, Improta G, Richetta M, De Santis R, Martorelli M. A further analysis on Ti6Al4V lattice structures manufactured by selective laser melting. *J Healthc Eng* 2019;2019.
- [10] Munford MJ, Xiao D, Jeffers JR. Lattice implants that generate homeostatic and remodeling strains in bone. *J Orthop Res* 2021;1–7.
- [11] Ghouse S, Reznikov N, Boughton OR, Babu S, Ng KC, Blunn G, et al. The design and in vivo testing of a locally stiffness-matched porous scaffold. *Appl Mater Today* 2019;15:377–88.
- [12] Frenzel T, Findeisen C, Kadic M, Gumbsch P, Wegener M. Tailored buckling microlattices as reusable light-weight shock absorbers. *Adv Mater* 2016;28(28):5865–70.
- [13] Gloria A, Montanari R, Richetta M, Varone A. Alloys for aeronautic applications: State of the art and perspectives. *Metals* 2019;9(6):662.
- [14] Wauthle R, Vrancken B, Beynaerts B, Jorissen K, Schrooten J, Kruth JP, et al. Effects of build orientation and heat treatment on the microstructure and mechanical properties of selective laser melted Ti6Al4V lattice structures. *Addit Manuf* 2015;5:77–84.
- [15] Ahmadi SM, Hedayati R, Li Y, Lietaert K, Tümer N, Fatemi A, et al. Fatigue performance of additively manufactured meta-biomaterials: The effects of topology and material type. *Acta Biomater* 2018;65:292–304.
- [16] Karami K, Blok A, Weber L, Ahmadi SM, Petrov R, Nikolic K, et al. Continuous and pulsed selective laser melting of Ti6Al4V lattice structures: Effect of post-processing on microstructural anisotropy and fatigue behaviour. *Addit Manuf* 2020;36:101433.
- [17] Ahmadi SM, Kumar R, Borisov EV, Petrov R, Leeftang S, Li Y, et al. From microstructural design to surface engineering: A tailored approach for improving fatigue life of additively manufactured meta-biomaterials. *Acta Biomater* 2019;83:153–66.
- [18] Pyka G, Burakowski A, Kerckhofs G, Moesen M, Van Bael S, Schrooten J, et al. Surface modification of Ti6Al4V open porous structures produced by additive manufacturing. *Adv Energy Mater* 2012;14(6):363–70.
- [19] Van Hooreweder B, Kruth JP. Advanced fatigue analysis of metal lattice structures produced by selective laser melting. *CIRP Ann - Manuf Technol* 2017;66(1):221–4.
- [20] Rathore JS, Vienne C, Quinsat Y, Tournier C. Influence of resolution on the X-ray CT-based measurements of metallic AM lattice structures. *Weld World* 2020;64(8):1367–76.
- [21] Du Plessis A, Yadroitsev I, Yadroitsava I, Le Roux SG. X-Ray microcomputed tomography in additive manufacturing: A review of the current technology and applications. *3D Print Addit Manuf* 2018;5(3):227–47.
- [22] Kerckhofs G, Pyka G, Moesen M, Schrooten J, Wevers M. High-resolution micro-CT as a tool for 3D surface roughness measurement of 3D additive manufactured porous structures. In: *Proceedings ICT 2012, international conference on industrial computed tomography*. 2012, p. 77–83.
- [23] Kerckhofs G, Pyka G, Moesen M, Van Bael S, Schrooten J, Wevers M. High-resolution microfocus X-Ray computed tomography for 3D surface roughness measurements of additive manufactured porous materials. *Adv Energy Mater* 2013;15(3):153–8.

- [24] Hossain U, Ghouse S, Nai K, Jeffers J. Mechanical and morphological properties of additively manufactured SS316L and Ti6Al4V micro-struts as a function of build angle. *Addit Manuf* 2021;46:102050.
- [25] Bültmann J, Merkt S, Hammer C, Hinke C, Prah U. Scalability of the mechanical properties of selective laser melting produced micro-struts. *J Laser Appl* 2015;27(S2):S29206.
- [26] Li P. Constitutive and failure behaviour in selective laser melted stainless steel for microlattice structures. *Mater Sci Eng A* 2015;622:114–20.
- [27] Ghouse S, Babu S, Nai K, Hooper PA, Jeffers JR. The influence of laser parameters, scanning strategies and material on the fatigue strength of a stochastic porous structure. *Addit Manuf* 2018;22:290–301.
- [28] MATLAB - MathWorks - MATLAB & Simulink.
- [29] Fang Q, Boas DA. Tetrahedral mesh generation from volumetric binary and grayscale images. In: *Proceedings - 2009 IEEE international symposium on biomedical imaging: From nano to macro*. 2009, p. 1142–5.
- [30] iso2mesh: a Matlab/Octave-based mesh generator, <http://iso2mesh.sourceforge.net/cgi-bin/index.cgi?Home>.
- [31] Schindelin J, Arganda-Carreras I, Frise E, Kaynig V, Longair M, Pietzsch T, et al. Fiji: AN open-source platform for biological-image analysis. *Nat Methods* 2012;9(7):676–82.
- [32] International Organization for Standardization. ISO 25178-2:2012 geometrical product specifications (GPS) — Surface texture: Areal part 2: Terms, definitions and surface texture parameters. 2012.
- [33] Persenot T, Burr A, Dendievel R, Buffière JY, Maire E, Lachambre J, et al. Fatigue performances of chemically etched thin struts built by selective electron beam melting: Experiments and predictions. *Materialia* 2020;9(January):100589.
- [34] Lozanovski B, Downing D, Tino R, du Plessis A, Tran P, Jakeman J, et al. Non-destructive simulation of node defects in additively manufactured lattice structures. *Addit Manuf* 2020;36:101593.
- [35] Lozanovski B, Downing D, Tino R, Tran P, Shidid D, Emmelmann C, et al. Image-based geometrical characterization of nodes in additively manufactured lattice structures. *3D Print Addit Manuf* 2021;8(1): 51–68.